ULTRASONIC WAVE AND TRANSDUCER MODELING WITH THE FINITE INTEGRATION TECHNIQUE (FIT)

René Marklein*
University of Kassel, Department of Electrical Engineering/Computer Science, Electromagnetic Field Theory, Wilhelmshöher Allee 71, D-34121 Kassel, Germany

Abstract — This paper presents in a unified way numerical methods for the time-domain modeling of ultrasonic waves and coupled ultrasonic-electromagnetic transducers. The modeling tools are based on the direct discretization of underlying governing field equations in integral form by applying the so-called finite integration technique on a staggered grid complex in space and time. This yields discrete grid equations, which can be written in matrix form introducing well-defined discrete topological matrix operators. These operators allow a consistent formulation of the discrete grid equations insuring the properties of the governing equations. The simple structure of the discrete grid equations allows a very efficient implementation on high performance computers, workstations, personal computers and even state-of-the-art laptops. The potential of the numerical codes is presented for selected applications, where the paper mainly focuses on applications in ultrasonic non-destructive evaluation.

I. INTRODUCTION

The computational time-domain modeling of different types of wave field problems is utilized in various disciplines of engineering and science: in increasingly challenging problems in remote sensing, communication, optics, geophysical exploration, ground penetrating radar, medical diagnosis, and non-destructive evaluation. For example, for the computer simulation of ultrasonic wave phenomena and transducers there is a need of simple, flexible, and powerful numerical methods. Figure 1 displays a typical sketch of a setup used in non-destructive testing with ultrasound and Figure 2 shows a typical transient echo signal measured with this setup.

Various numerical techniques can be applied today to model transient ultrasonic waves and transducers: for instance, the finite difference (FD), finite element (FE), finite volume (FV), finite difference time domain (FDTD), finite integration (FI), and finite volume time domain (FVTD) method.

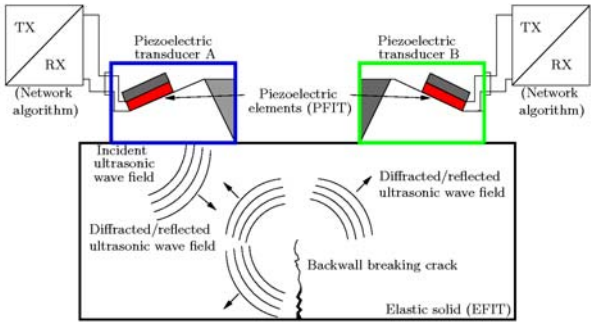

Figure 1: Typical setup applied in non-destructive testing with ultrasonic waves: steel block with a perfect scatterer.

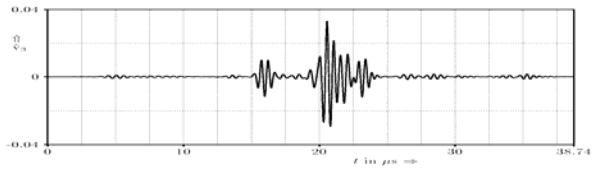

Figure 2: Typical time history of a transient echo signal (A-Scan) received in pulse-echo mode.

In this paper we present in a unified way the application of the finite integration technique (FIT) for the time-domain modeling of ultrasonic waves and coupled ultrasonic-electromagnetic transducers. The presented numerical modeling tools are called AFIT, EFIT, PFIT, and EMUSFIT, which stands for acoustic (A), elastodynamic (E), piezoelectric (P), and electromagnetic-ultrasonic (EMUS) finite integration technique (FIT).

Historically, the FIT has been introduced three decades ago in electrodynamics [1], where the FIT is applied to the full set of Maxwell's equations in integral form. Then, these ideas were adapted to the elastodynamics, which resulted in the so-called elastodynamic finite integration technique (EFIT) [2]. A unified treatment of the acoustic, electromagnetic, elastodynamic, piezoelectric, and electromagnetic-ultrasonic case can be found in [3, 4] and applications are given for instance in [2-6].

II. Governing Field Equations For Ultrasonic Waves and Ultrasonic Transducer Modeling

Ultrasonic Wave Modeling with AFIT and EFIT

The governing field equations for the ultrasonic wave modeling are the linear equations of acoustics and elastodynamics, which read for linear, inhomogeneous, anisotropic, instantaneously and locally reacting media in integral form:

(Acoustics)

$$\iiint_V \underline{\mathbf{j}}(\underline{\mathbf{R}},t)dV = -\oiint_{S=\partial V} \underline{\mathbf{n}}\, p(\underline{\mathbf{R}},t)dS + \iiint_V \underline{\mathbf{f}}(\underline{\mathbf{R}},t)dV \quad (1)$$

$$\iiint_V \dot{S}(\underline{\mathbf{R}},t)dV = \oiint_{S=\partial V} \underline{\mathbf{n}}\bullet\underline{\mathbf{v}}(\underline{\mathbf{R}},t)dS + \iiint_V h(\underline{\mathbf{R}},t)dV \quad (2)$$

(Elastodynamics)

$$\iiint_V \underline{\mathbf{j}}(\underline{\mathbf{R}},t)dV = \oiint_{S=\partial V} \underline{\mathbf{n}}\bullet\underline{\underline{\mathbf{T}}}(\underline{\mathbf{R}},t)dS + \iiint_V \underline{\mathbf{f}}(\underline{\mathbf{R}},t)dV \quad (3)$$

$$\iiint_V \dot{\underline{\underline{\mathbf{S}}}}(\underline{\mathbf{R}},t)dV = \oiint_{S=\partial V} \mathrm{sym}\{\underline{\mathbf{n}}\,\underline{\mathbf{v}}(\underline{\mathbf{R}},t)\}\, dS + \iiint_V \underline{\underline{\mathbf{h}}}(\underline{\mathbf{R}},t)dV \quad (4)$$

p	[N/m^2]	Pressure
$\underline{\mathbf{j}}$	[Ns/m^3]	Momentum density vector
$\underline{\mathbf{v}}$	[m/s]	Particle velocity vector
S	[1]	Scalar deformation
$\underline{\mathbf{f}}$	[N/m^3]	Volume force density vector
h	[1/s]	Injected deformation rate
$\underline{\underline{\mathbf{T}}}$	[N/m]	Cauchy's stress tensor
$\underline{\mathbf{j}}$	[Ns/m^3]	Momentum density vector
$\underline{\mathbf{v}}$	[m/s]	Particle velocity vector
$\underline{\underline{\mathbf{S}}}$	[1]	Deformation tensor
$\underline{\mathbf{f}}$	[N/m^3]	Volume force density vector
$\underline{\underline{\mathbf{h}}}$	[1/s]	Injected deformation rate tensor

In the above Equations (1)-(4) $S=\partial V$ is the closed surface of the volume V and $\underline{\mathbf{n}}$ is the outward unit vector of S. The symmetric part of a second rank tensor is denoted by $\mathrm{sym}\{\underline{\mathbf{n}}\underline{\mathbf{v}}(\underline{\mathbf{R}},t)\} = \frac{1}{2}\left\{\underline{\mathbf{n}}\underline{\mathbf{v}}(\underline{\mathbf{R}},t)+[\underline{\mathbf{n}}\underline{\mathbf{v}}(\underline{\mathbf{R}},t)]^{21}\right\}$.

The Equations (1)-(4) are coupled if we introduce appropriate constitutive equations, e.g., for linear, inhomogeneous, anisotropic, instantaneously and locally reacting media:

(Acoustics)

$$\underline{\mathbf{j}}(\underline{\mathbf{R}},t) = \rho_{a0}(\underline{\mathbf{R}})\underline{\mathbf{v}}(\underline{\mathbf{R}},t) \quad (4)$$

$$S(\underline{\mathbf{R}},t) = -\kappa(\mathbf{R})\, p(\underline{\mathbf{R}},t) \quad (5)$$

(Elastodynamics)

$$\underline{\mathbf{j}}(\underline{\mathbf{R}},t) = \rho_{e0}(\underline{\mathbf{R}})\underline{\mathbf{v}}(\underline{\mathbf{R}},t) \quad (6)$$

$$\underline{\underline{\mathbf{S}}}(\underline{\mathbf{R}},t) = \underline{\underline{\underline{\underline{\mathbf{s}}}}}(\mathbf{R}) : \underline{\underline{\mathbf{T}}}(\underline{\mathbf{R}},t) \quad (7)$$

ρ_{a0}	[kg/m^3]	Acoustic mass density at rest
κ	[m^2/N]	Compressibility
ρ_{e0}	[kg/m^3]	Elastic mass density at rest
$\underline{\underline{\underline{\underline{\mathbf{s}}}}}$	[m^2/N]	Compliance tensor of rank four

If we add appropriate time integration schemes to the two sets of equations and apply the finite integration technique (FIT) using a staggered grid complex in space and time, we obtain the following two sets of matrix equations:

(Acoustics)

$$\{\dot{\mathbf{v}}\}^{(n_t-\frac{1}{2})} = [\tilde{\boldsymbol{\rho}}_{a0}]^{-1}\{[\widetilde{\mathbf{R}}]^{-1}[\widetilde{\mathbf{grad}}]\{\mathbf{p}\}^{(n_t-\frac{1}{2})} + \{\mathbf{f}\}^{(n_t-\frac{1}{2})}\} \quad (8)$$

$$\{\mathbf{v}\}^{(n_t)} = \{\mathbf{v}\}^{(n_t-1)} + \Delta t\{\dot{\mathbf{v}}\}^{(n_t-\frac{1}{2})} \quad (9)$$

$$\{\dot{\mathbf{p}}\}^{(n_t)} = -[\boldsymbol{\kappa}]^{-1}[\mathbf{div}][\mathbf{R}]^{-1}\{\mathbf{v}\}^{(n_t)} - [\boldsymbol{\kappa}]^{-1}\{\mathbf{h}\}^{(n_t)} \quad (10)$$

$$\{\mathbf{p}\}^{(n_t+\frac{1}{2})} = \{\mathbf{p}\}^{(n_t-\frac{1}{2})} + \Delta t\{\dot{\mathbf{p}}\}^{(n_t)} \quad (11)$$

(Elastodynamics)

$$\{\dot{\mathbf{v}}\}^{(n_t-\frac{1}{2})} = [\tilde{\boldsymbol{\rho}}_{e0}]^{-1}\{[\widetilde{\mathbf{DIV}}][\widetilde{\mathbf{R}}_{\dot{\mathbf{v}}}^{\mathrm{T}}][\mathbf{A}_{\dot{\mathbf{v}}}^{\mathrm{T}}]\{\mathbf{T}\}^{(n_t-\frac{1}{2})} + \{\mathbf{f}\}^{(n_t-\frac{1}{2})}\} \quad (12)$$

$$\{\mathbf{v}\}^{(n_t)} = \{\mathbf{v}\}^{(n_t-1)} + \Delta t\{\dot{\mathbf{v}}\}^{(n_t-\frac{1}{2})} \quad (13)$$

$$\{\dot{\mathbf{T}}\}^{(n_t)} = [\mathbf{c}][\mathbf{R}_{\dot{\mathbf{T}}}^{\mathrm{v}}]^{-1}[\mathbf{GRAD}][\mathbf{A}_{\dot{\mathbf{T}}}^{\mathrm{v}}]\{\mathbf{v}\}^{(n_t)} + \{\mathbf{g}\}^{(n_t)} \quad (14)$$

$$\{\mathbf{T}\}^{(n_t+\frac{1}{2})} = \{\mathbf{T}\}^{(n_t-\frac{1}{2})} + \Delta t\{\dot{\mathbf{T}}\}^{(n_t)}. \quad (15)$$

These are the so-called grid equations of AFIT and EFIT in matrix form, which represent a one-to-one translation to the governing equations. Each of the above two sets of matrix equations represents an explicit marching-on-in-time algorithm of "leap frog" type of second order in space and time.

The topological operators are ensuring essential vector analytic properties in the discrete grid space:

$$\nabla\times\nabla = \underline{\mathbf{0}} \Leftrightarrow [\mathbf{curl}][\mathbf{grad}] = [\widetilde{\mathbf{curl}}][\widetilde{\mathbf{grad}}] = [\mathbf{0}] \quad (16)$$

$$\nabla\bullet\nabla\times = 0 \Leftrightarrow [\mathbf{div}][\mathbf{curl}] = [\widetilde{\mathbf{div}}][\widetilde{\mathbf{curl}}] = [\mathbf{0}], \quad (17)$$

where the algebraic null matrix is denoted by $[\mathbf{0}]$.

Further details are given in [3, 4] and modeling results can be found in [2-6].

Ultrasonic Transducer Modeling with PFIT and EMUSFIT

The piezoelectric finite integration technique (PFIT) and the electromagnetic-ultrasonic finite integration technique (EMUSFIT) are time-domain modeling tools for typical transducers applied in ultrasonics [3, 4]. Due to the limited space, in the following we only consider the piezoelectric case. The constitutive relations for piezoelectric materials read for linear, inhomogeneous, instantaneously and locally reacting piezoelectric (pe) media:

$$\underline{\mathbf{D}}(\underline{\mathbf{R}},t) = \underline{\underline{\boldsymbol{\varepsilon}}}^{\mathrm{S}}(\underline{\mathbf{R}})\bullet\underline{\mathbf{E}}(\underline{\mathbf{R}},t) + \underline{\underline{\underline{\mathbf{e}}}}_{\mathrm{pe}}(\underline{\mathbf{R}}) : \underline{\underline{\mathbf{S}}}(\underline{\mathbf{R}},t) \tag{18}$$

$$\underline{\underline{\mathbf{S}}}(\underline{\mathbf{R}},t) = [\underline{\underline{\underline{\mathbf{d}}}}_{\mathrm{pe}}(\underline{\mathbf{R}})]^{231}\bullet\underline{\mathbf{E}}(\underline{\mathbf{R}},t) + \underline{\underline{\underline{\mathbf{s}}}}^{\mathrm{E}}(\underline{\mathbf{R}}) : \underline{\underline{\mathbf{T}}}(\underline{\mathbf{R}},t)\,. \tag{19}$$

$\underline{\underline{\boldsymbol{\varepsilon}}}^{\mathrm{S}}$	[As/Vm]	Permittivity tensor at $\underline{\underline{\mathbf{S}}}$ = const.
$\underline{\underline{\underline{\mathbf{e}}}}_{\mathrm{pe}}$	As/m^2]	Piezoelectric coupling tensor of third rank
$\underline{\underline{\underline{\mathbf{s}}}}^{\mathrm{E}}$	[m^2/N]	Compliance tensor at $\underline{\mathbf{E}}$ = const.
$\underline{\underline{\underline{\mathbf{d}}}}_{\mathrm{pe}}$	[As/N]	Piezoelectric coupling tensor of third rank

If we assume that the typical dimension of the piezoelectric material is small compared to the electromagnetic wavelength - low frequency approximation for Maxwell's equations -, we can neglect the induction term in Faraday's law. Then, the electric field strength is an irrotational gradient field, i.e., $\underline{\mathbf{E}}(\underline{\mathbf{R}},t) = -\nabla\Phi(\underline{\mathbf{R}},t)$ with the scalar electric potential $\Phi(\underline{\mathbf{R}},t)$, where $\nabla\times\underline{\mathbf{E}}(\underline{\mathbf{R}},t) = \underline{\mathbf{0}}$ holds. This is the so-called electroquasistatic (EQS) approximation [3]. This results in an elliptic Poisson equation for the time derivative of the scalar electric potential

$$\nabla\bullet\left[\underline{\underline{\boldsymbol{\varepsilon}}}^{\mathrm{S}}(\underline{\mathbf{R}})\bullet\nabla\frac{\partial}{\partial t}\Phi(\underline{\mathbf{R}},t)\right] = \nabla\bullet\underline{\underline{\underline{\mathbf{e}}}}_{\mathrm{pe}}(\underline{\mathbf{R}}) : \mathrm{sym}\{\nabla\underline{\mathbf{v}}(\underline{\mathbf{R}},\mathrm{t})\} - \frac{\partial}{\partial t}\rho_{\mathrm{e}}(\underline{\mathbf{R}},t). \tag{20}$$

The application of FIT to the integral form of Eq. (20) yields the following equation in matrix form

$$\begin{aligned}[\widetilde{\mathbf{div}}][\tilde{\mathbf{S}}][\tilde{\boldsymbol{\varepsilon}}^{\mathrm{S}}][\mathbf{R}]^{-1}[\mathbf{grad}]\{\dot{\boldsymbol{\Phi}}\}^{(n_t)} &= [\widetilde{\mathbf{div}}][\tilde{\mathbf{S}}][\tilde{\mathbf{e}}_{\mathrm{pe}}][\mathbf{R}^{\mathrm{v}}_{\Phi}]^{-1}[\mathbf{GRad}][\mathbf{A}^{\mathrm{v}}_{\Phi}]\{\mathbf{v}\}^{(n_t)} \\ &\quad -[\mathbf{V}^{\dot{\rho}}_{\Phi}]\{\dot{\boldsymbol{\rho}}_{\mathrm{e}}\}^{(n_t)} - [\mathbf{S}^{\dot{\eta}}_{\Phi}]\{\dot{\boldsymbol{\eta}}_{\mathrm{e}}\}^{(n_t)}\end{aligned} \tag{21}$$

with $[\mathbf{curl}]\{\mathbf{E}\}^{(n_t)} = \{\mathbf{0}\}$ and $\{\mathbf{E}\}^{(n_t)} = -[\mathbf{R}]^{-1}[\mathbf{grad}]\{\boldsymbol{\Phi}\}^{(n_t)}$.

The underlying staggered grid complex in space and time of PFIT is displayed in Figure 3. PFIT uses a scalar electric potential-velocity-stress formulation.

a)

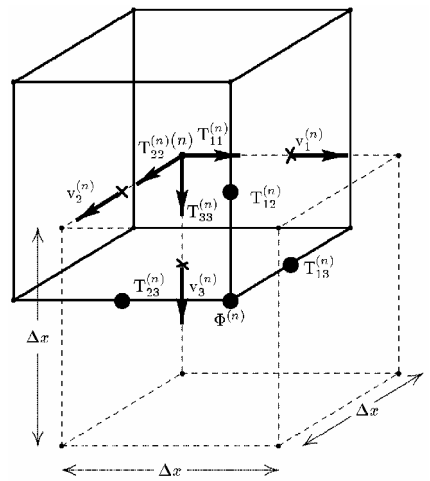

b)

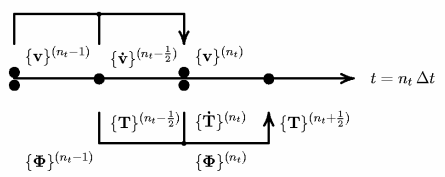

Figure 3: Staggered spatial (a) and staggered temporal (b) grid complex of PFIT.

PFIT comes in two versions, a voltage and a current driven version, U- and I-PFIT [3]. The I-PFIT can be combined with a 1-D network algorithm to model an external impedance load (see Fig. 4).

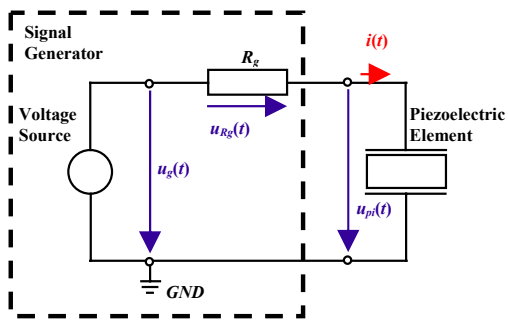

Figure 4: Equivalent circuit modeled by a 1-D network algorithm.

Figure 5 and 6 show the PFIT modeling of a piezoelectric transducer coupled to a solid brass cylinder with a backwall breaking notch. A comparison between the modeled and experimental

piezoelectric voltage observed at the piezoelectric disk is given in Fig. 5, displaying the agreement between the numerical and physical world. The dominant echo signals are the excitation pulse, the notch echo, and the backwall echo. Time-domain snapshots are displayed in Fig. 6, which show the ultrasonic wave propagation and the generation of the so-called notch echo signal and backwall echo signal.

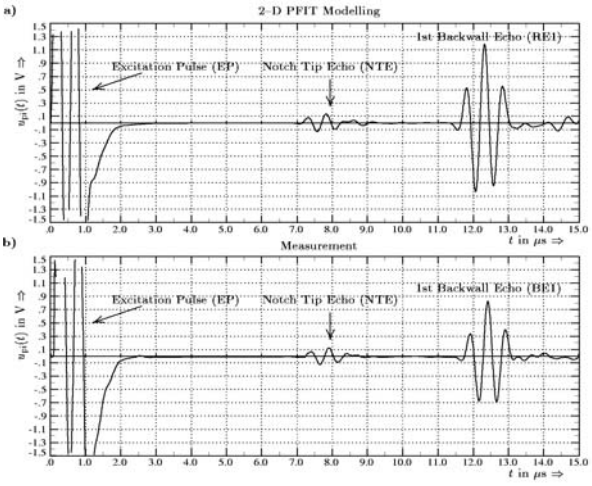

Figure 5: Pz27 disk on a brass cylinder with a backwall breaking notch: comparison between the numerical (a) and experimental (b) piezoelectric voltage at the Pz27 disk for an external impedance load of R_g = 50 Ω; two cycle sine pulse excitation with u_0 = 10 V and f_c = 2 MHz.

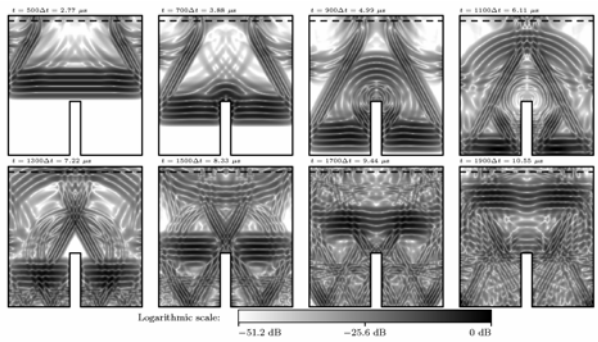

Figure 6: Pz27 disk on a brass cylinder with a backwall breaking notch: 2-D PFIT time-domain snapshots of the magnitude of the particle velocity vector.

III. Conclusion

The paper presented the application of the finite integration technique in ultrasonic wave and transducer modeling, e.g., piezoelectric transducers. Especially, the paper tried to present the topic under consideration in a unified way starting from the sets of field and constitutive relations up to the sets of discrete grid equations. This unified presentation gives a deep insight into the physical similarities between the different phenomena and their numerical treatment.

Due to the limited space and the various wave field phenomena it is impossible to cover all features of the finite integration technique and its application in time-domain computation of wave fields. The author refers to the references below and references therein.

IV. References

[1] T. Weiland, "A Discretization Method for the Solution of Maxwell's Equations for Six-component Fields," Electron. Commun. (AEÜ), vol. 31, no. 3, pp. 116-120, 1977.

[2] P. Fellinger, R. Marklein, K. J. Langenberg, and S. Klaholz, "Numerical modeling of elastic wave propagation and scattering with EFIT - elastodynamic finite integration technique," Wave Motion, vol. 21, pp. 47-66, 1995.

[3] R. Marklein, Numerical Methods for the Modeling of Acoustic, Electromagnetic, Elastic and Piezoelectric Wave Propagation Problems in the Time Domain Based on the Finite Integration Technique, Shaker Verlag, Aachen, 1997. (in German, available from http://www.shaker.de)

[4] R. Marklein, "The Finite Integration Technique as a General Tool to Compute Acoustic, Electromagnetic, Elastodynamic, and Coupled Wave Fields," in W. R. Stone (ed.), Review of Radio Science, 1999-2002 URSI, IEEE Press and John Wiley and Sons, pp. 201-244, 2002.

[5] K.-J. Langenberg, R. Marklein, K. Mayer, "Applications to Nondestructive Testing with Ultrasound," in E. R. Pike, P. C. Sabatier (eds.), Scattering, vol. 1, Academic Press, London, pp. 594-617, 2002.

[6] F. Schubert, R. Marklein, "Numerical Computation of Ultrasonic Wave Propagation In Concrete Using the Elastodynamic Finite Integration Technique (EFIT)", this volume.

Footnotes:

*René Marklein: marklein@uni-kassel.de and http://www.uni-kassel.de/fb16/tet/marklein